Journal of the European Ceramic Society **18** (1998) 737–744

PII: S0955-2219(97)00187-8
0955-2219/98/$19.00 + 0.00

Reaction Sequence in the Formation of Perovskite $Pb(ZrO_{0.48}Ti_{0.52})O_3$–$Pb(Nb_{2/3}Ni_{1/3})O_3$ Solid Solution: Dynamic Heat-Treatment

O. Babushkin,[a] T. Lindbäck,[a] J.-C. Luc[b] and J.-Y. M. Leblais[b]

[a]Division of Engineering Materials, Luleå University of Technology, S-971 87 Luleå, Sweden
[b]Quartz et Silice Research Institute, B.P. 95, F-77792 Nemours, France

(Received 28 April 1997; accepted 22 October 1997)

Abstract

The sequence of the solid state reactions in the PbO–ZrO_2–TiO_2–Nb_2O_5–NiO system has been investigated. The oxide mixing route utilised in sample preparation was selected in order to determine the basic reaction path in the formation of the PZT–PNN perovskite phase. It has been established that the main intermediate phases formed prior to PZT–PNN are $PbTiO_3$ and pyrochlore Pb–Nb–based phases. The sequence in the pyrochlore formation was from tetragonal $Pb_3Nb_2O_8$ (500°C) to rhombohedral $Pb_2Nb_2O_7$ (600–750°C) and finally to cubic $Pb_3Nb_4O_{13}$ (650–850°C). The formation of the perovskite phase proceeded from mutual solubility of $PbTiO_3$ and pyrochlore $Pb_3Nb_4O_{13}$ phases, accompanied by dissolving of residuals ($PbZrO_3$ and NiO) in the perovskite solid solution formed.

1 Introduction

Since 1954, when Joffe[1] reported the discovery of a piezoelectric ceramic based on the $Pb(Zr_xTi_{1-x})O_3$ (PZT) solid solution it has become one of the main commercially produced piezoelectric ceramic materials and is applied extensively in a wide range of fields. Nowadays, most practical piezoelectric ceramic materials are based on binary and ternary systems developed from PZT. The variation in composition is made possible by the nature of perovskites, which permits different combinations of substitutions in the A and B sites of the ABO_3 structure. The additives can be isovalent or aliovalent, and the charge imbalance restored by generating vacancies in cationic or anionic sites. Thus use of different dopants has greatly extended the range of application of perovskites.

Of the various routes available to prepare bulk piezoelectric oxides the pure constituent oxide mixing route is of continuing interest, particularly with regard to reducing the variability of the dielectric and electromechanical properties which can be caused by differences in processing and precursors. The work described here is devoted to investigations of solid-state reactions taking place during the calcination stage in the PbO–ZrO_2–TiO_2–Nb_2O_5–NiO system. This system is the basis for sintering of the $Pb(ZrO_{0.48}Ti_{0.52})O_3$–$Pb(Nb_{2/3}Ni_{1/3})O_3$ (PZT–PNN) solid solution. The main aim of the work is to gain knowledge of the basic sequence of solid state reactions in this mixture of oxides, rather than to examine mixed oxide routes with different precursors introduced at different precalcination stages.

2 Experimental Procedure.

A perovskite solid solution of the stoichiometric composition $Pb(Ti_{0.48}Zr_{0.52})O_3$–$Pb(Nb_{2/3}Ni_{1/3})O_3$ (PZT–PNN) was chosen as the basis of the investigation. The constituent oxides were reagent-grade powders of PbO (yellow), titanium dioxide (TiO_2), niobium pentoxide (Nb_2O_5), zirconium dioxide (ZrO_2) and nickel oxide (NiO). (Table 1). These were characterised by determining their as-received surface areas and particle sizes. Two mixtures (here referred to as Z1 and Z2) were prepared differing only in the form of the ZrO_2 used. The two ZrO_2

Table 1. Purity and particle size of the precursors

No.	*Constituent*	*Purity (%)*	*Particle size ($m^2 g^{-1}$)*
1	PbO	99·9	0·6
2	TiO_2	99·9	19·1
3	NiO	99·0	1·0
4	Nb_2O_5	99·9	2·1
5	ZrO_2	99·9	7·0
6	ZrO_2 (activated)	99·9	25·0

All powders were supplied by Quartz and Silice.

powders had specific surface areas $7\,m^2 g^{-1}$ and $25\,m^2 g^{-1}$ respectively, the latter being referred to as an activated powder.

The two slurries with the weight proportions of the PZT–PNN and differing only in the ZrO_2 powder used were blended for 5 h in a ball mill and then pan-dried. The mixtures were then granulated by passing through a sieve and pressed into pellets 15 mm in diameter and 2 mm thick, for calcination.

Dynamic calcination of the batch Z2 mixture was carried out at temperatures between 500 and 850°C, at intervals of 50°C. The heating rate was 250°C h^{-1} with a soaking time of 5 min at the selected calcination temperature. Samples were then taken from the furnace and quenched in air on a water-cooled plate. Special isothermal treatment with different soaking times between 2 and 300 min at 850°C was undertaken for the Z1 and Z2 mixtures.

The compositions of the phases developed during calcination were examined by powder X-ray diffractometry on the as-quenched samples in a Philips PW-1710 automatic diffractometer with a step and a continuous scanning device. The diffractometer was equipped with a vertical goniometer PW 1050/25, graphite monochromator PW 1752/00, proportional counter for reflected beam PW 1711/10 and a PW 1730/25 generator. Diffraction patterns were measured in a 2Θ range of 10°–90° using Cu K_α radiation of 50 kV and 30 mA.

Quantitative analysis was performed on the diffraction patterns collected in a step scan mode. The quantitative evaluation was based on the assumption that the intensity of the diffraction peaks of a chemical compound are dependent on the structure and elements of the compound, the diffractometer characteristics, the weight fraction of the compound in the total sample, and the absorption coefficient of the sample.[2] This can be expressed as follows:

$$C_i = k_i I_i m \qquad (1)$$

Here C_i is the concentration or weight fraction of compound i; k_i is the calibration constant of the i-phase in the relevant diffractometer; I_i is the net intensity of a peak of compound i and m is the mass absorption coefficient of the sample (mixture of compounds). By definition, eqn (1) embodies the following simplifications: (a) the overall chemical composition of the investigated mixtures is constant and (b) the mass absorption coefficients of a mixture and the mass absorption coefficients of the constituents of this mixture are approximately equal or differ by no more than 15%. In this case the unknown constant k_i can be cancelled out if the intensity of a selected diffraction line of the investigated phase is divided by a standard reference line. Here, in the external standard method, the intensity of a selected peak of the investigated phase in the mixture is compared with the intensity of the same peak of the pure phase. Hence the intensity ratio depends only on the weight fraction of the phase i in the mixture and the absorption coefficients of the mixture and pure i-phase. For this purpose binary phases $PbTiO_3$, $Pb_2Nb_2O_7$, $Pb_3Nb_4O_{13}$ and $PbZrO_3$ were sintered as standards.

Semiquantitative estimates of the effective crystallite size were obtained based on X-ray line broadening measurements of the (220) PZT–PNN perovskite peak using the (110) reflection of tungsten as an external standard. The profiles were obtained as step scans using a step size of 0·02°2 Θ and count times of 8 s. The profiles were corrected for background and $K\alpha$ prior to analysis. Accurate assignment of the peak positions was facilitated by fitting with a non-linear Marquardt least-squares routine that accounts for the K_α splitting. The lattice parameters of the PZT–PNN solid solution formed were refined by application of a least-squares refinement program.

Thin layers of powdered samples were spread on metallic substrates for investigation by scanning electron microscopy (SEM) in a Philips XL 30 microscope.

3 Results

3.1 XRD phase analysis

Analysis of solid state reactions and phase transformations taking place during the calcination is considered in three temperature intervals: 500–600°C, 600–700°C, 700–850°C, and at 850°C for soaking times between 2 and 300 min.

3.1.1 Temperature interval 500–600°C

Polymorphic phase transformations, as well as the formation of new phases were observed within this temperature range. The transformation of two metastable forms of lead oxide namely litharge and minium to the stable massicot form occurred at temperatures 500 and 550°C (Figs 1 and 2). At 600°C, the transformation of these phases was

complete, as is suggested by the absence of their main peaks. The formation of new phases based on $PbTiO_3$ and pyrochlore was observed at 500–550°C (Figs 1 and 2). The formation of $PbTiO_3$ was accompanied by a marked reduction in the intensity of the TiO_2 main peak at 600°C. The formation of the Nb-based pyrochlore phase proceeded through an initial precipitation of tetragonal Pb-rich $Pb_3Nb_2O_8$ phase leading to the pyrochlore rhombohedral $Pb_2Nb_2O_7$-based phase at 600°C and above.

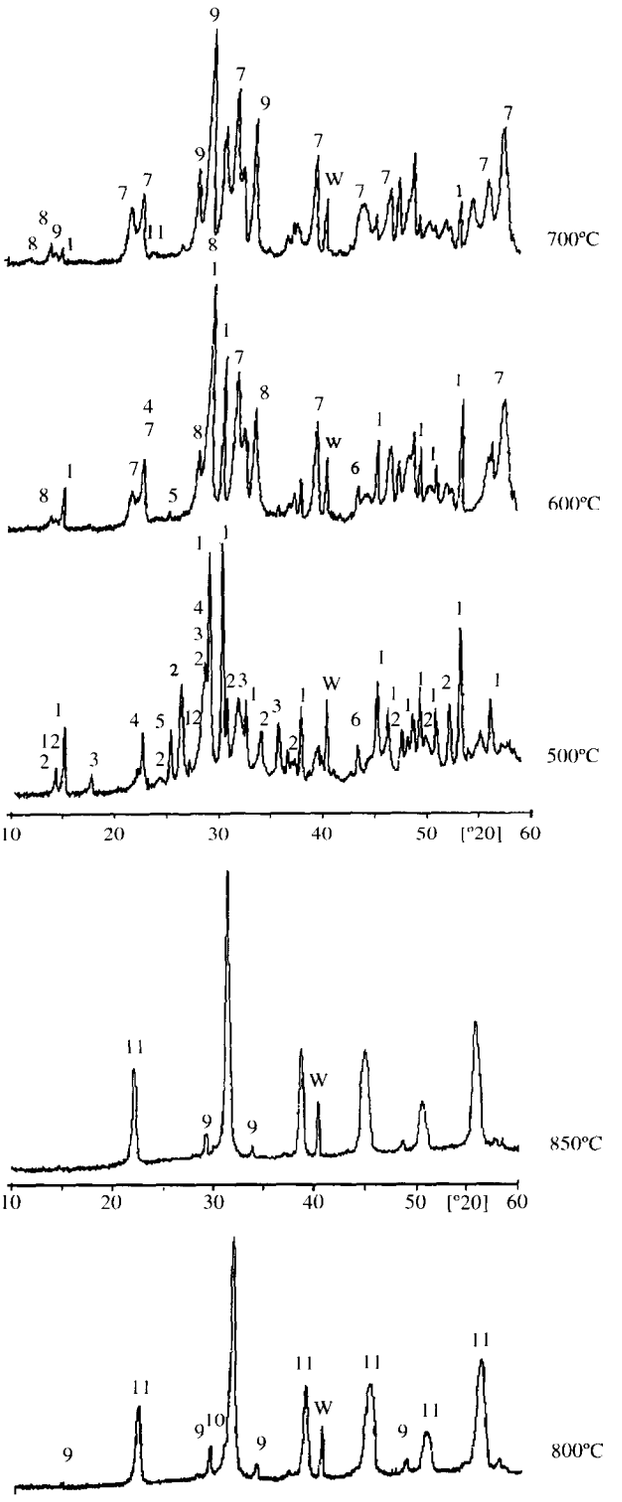

Fig. 1. X-ray diffraction patterns of the samples treated at different temperatures for 300 min. Where: 1, PbO (massicot); 2, Pb_3O_4; 3, PbO (litharge); 4, Nb_2O_5; 5, TiO_2; 6, NiO; 7, $PbTiO_3$; 8, $Pb_2Nb_2O_7$; 9, $Pb_3Nb_4O_{13}$; 10, $PbZrO_3$; 11, PZT–PNN (perovskite); 12, $Pb_3Nb_2O_8$ and W, (standard).

3.1.2 Temperature interval 600–700°C

Within this temperature interval the phase composition was characterised by further development of the two main phases based on $PbTiO_3$ and the pyrochlore, rhombohedral $Pb_2Nb_2O_7$. At the same time the first traces of a new high temperature cubic pyrochlore phase based on $Pb_3Nb_4O_{13}$ were observed at 650°C. The formation of a new $PbZrO_3$ phase was also found at this temperature. The residual PbO phase content continued to decrease (Figs 1 and 2) but the residual NiO did not react within this temperature interval as indicated by the constant intensity of the main (200) NiO peak.

3.1.3 Temperature interval 700–850°C

This temperature interval was characterised by the formation of the main PNN based solid solution. Traces of the phase were already indicated at 750°C and a sharp increase was observed at 800°C. The residual $PbTiO_3$ was rapidly dissolved and only very weak peaks of this phase were observed at 800°C (Figs 1 and 2). The amount of cubic pyrochlore phase and $PbZrO_3$ was drastically reduced above 700°C but small traces were still detectable at 850°C. The residual PbO was completely dissolved at 750°C and NiO was not detected over 800°C.

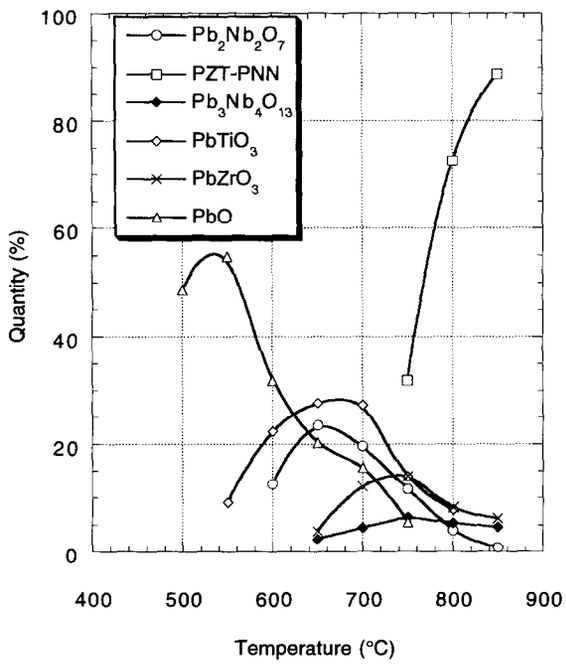

Fig. 2. Quantities of main phases as a function of temperature.

3.1.4 Soaking time 2–300 min at 850°C

Special attention was paid to a comparison of the solid state reactions in the two mixtures, Z1 and Z2, containing different grades of ZrO_2 powder. Diffraction patterns of the quenched samples indicated sharp and well developed symmetrical profiles that could be referred to the pseudocubic PZT–PNN based solid solution. The amount of perovskite phase increased progressively with increasing soaking time. The amount of this phase finally attained was 93 wt% in the Z1 mixture and 98 wt% in the Z2 mixture [Fig. 3(a)]. At the same time the diffractograms showed in both cases remaining traces of the cubic pyrochlore phase even after 5 h soaking time. Quantitative evaluation showed that the concentration of this residual phase was at an acceptably low level, being estimated at 3·5 wt% for Z1 and 2·0 wt% for Z2 after 5 h soaking time [Fig. 3(b)]. The other residual phase, PbZrO3, was observed at the beginning of exposure at 850°C, but in the Z2 mixture was completely dissolved (not detectable by X-ray diffraction) within 180 min soaking time. In samples based on batch Z1 (i.e. non activated ZrO_2), traces of $PbZrO_3$ were detected even after 300 min soaking time and estimated at approximately 3·5 wt% [Fig. 3(b)]. In summary, it can be concluded that after the calcination the final phase composition in both cases was the perovskite based PZT–PNN solid solution with traces of cubic pyrochlore $Pb_3Nb_4O_{13}$ phase [Fig. 3(a) and (b)]. The Z1 mixture utilising non-activated zirconia also contained residual traces of $PbZrO_3$. It seems that for the conventional oxide route process, the 850°C, 5 h calcination is not sufficient to eliminate the pyrochlore phase.

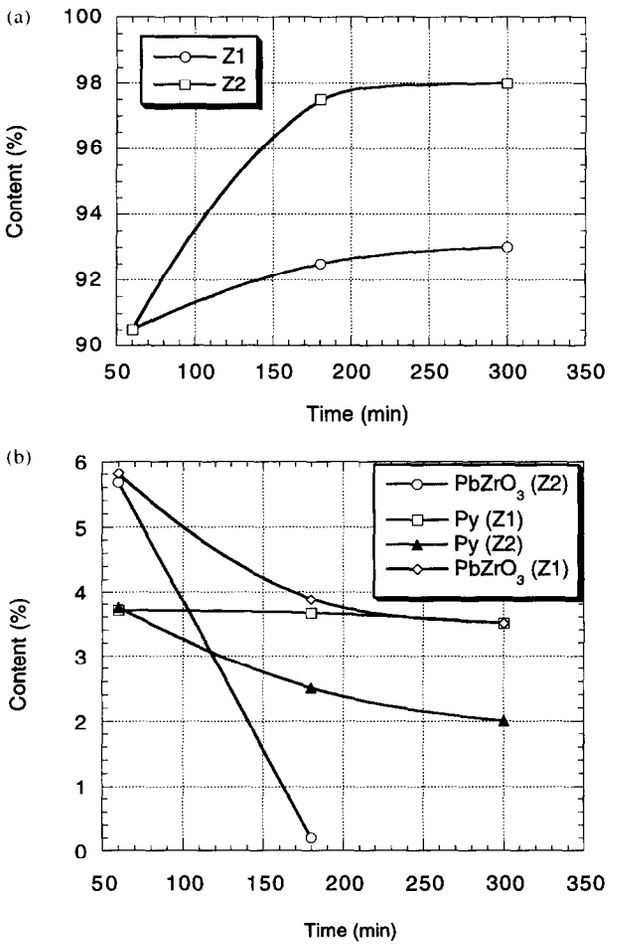

Fig. 3. Quantity of (a) the perovskite phase and (b) residual phases versus soaking time at 850°C for the batches Z1 and Z2.

3.2 Structure analysis of the perovskite phase

Unit cell analysis of the perovskite structure was performed on the basis of an assumed pseudocubic cell. The step scans and subsequent crystal structure analysis were performed in association with an external standard of annealed analytical grade tungsten powders. The first eight reflections accepted for least square refinement of the cubic unit cell were 100; 110; 111; 200; 210; 211; 220 and 300. The analysis revealed a systematic increase of cell dimension with increasing soaking time [Table 2, Fig. 4(a)].

In addition to the above calculation of lattice parameters a profile analysis was made of the (220) peak with respect to full width at half-maximum (FWHM). The computed values revealed a continuous decrease of FWHM, up to 14% for mixture Z2 and 4% for mixture Z1. [Fig. 4(b)]. Application of the Scherrer equation[2] to calculate the domain or particle size revealed, as expected, pronounced growth in batch Z2, the particle size changing from 155 nm after 60 min to 500 nm after 300 min soaking time [Fig. 4(c)]. In batch Z1, the particle size changed only slightly from 60 nm (60 min) to 80 nm (300 min).

3.3 Microstructure

Evaluation of the microstructure of the calcined samples was performed by SEM examination of gently pulverised samples spread thinly on metallic substrates. This showed that all the particles had an irregular shape and were agglomerated. On surfaces of the matrix grains, small precipitates can be seen (Fig. 5). These precipitates can be referred to the residual pyrochlore phase. Estimation of the particle size from the SEM image yielded values

Table 2. Lattice parameters of the perovskite pseudocubic phase

Time (min)	a_{Z1} (Å)	a_{Z2} (Å)
60	4·03461 ± 0·00085	4·03325 ± 0·00069
180	4·03640 ± 0·00078	4·03718 ± 0.00068
300	4·03743 ± 0.00069	4·03803 ± 0·00036

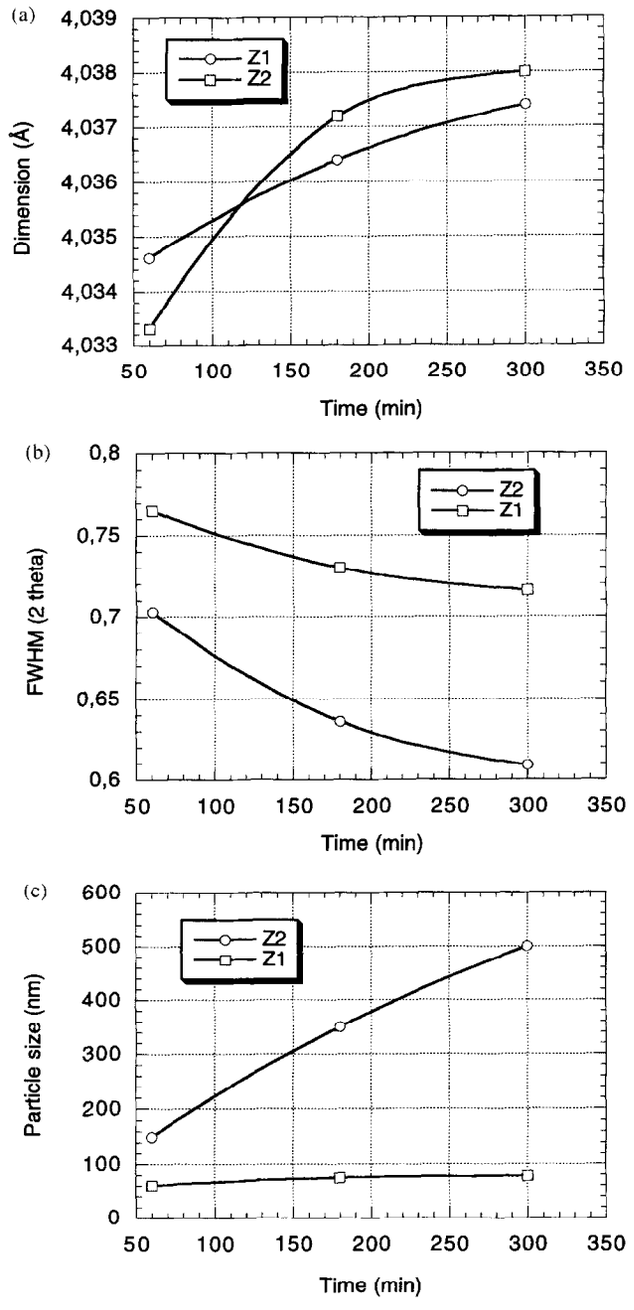

Fig. 4. (a) the perovskite particle sizes and (b) FWHM of the (220) perovskite peak and (c) lattice dimensions of the perovskite pseudocubic phase for samples of batches Z1 and Z2.

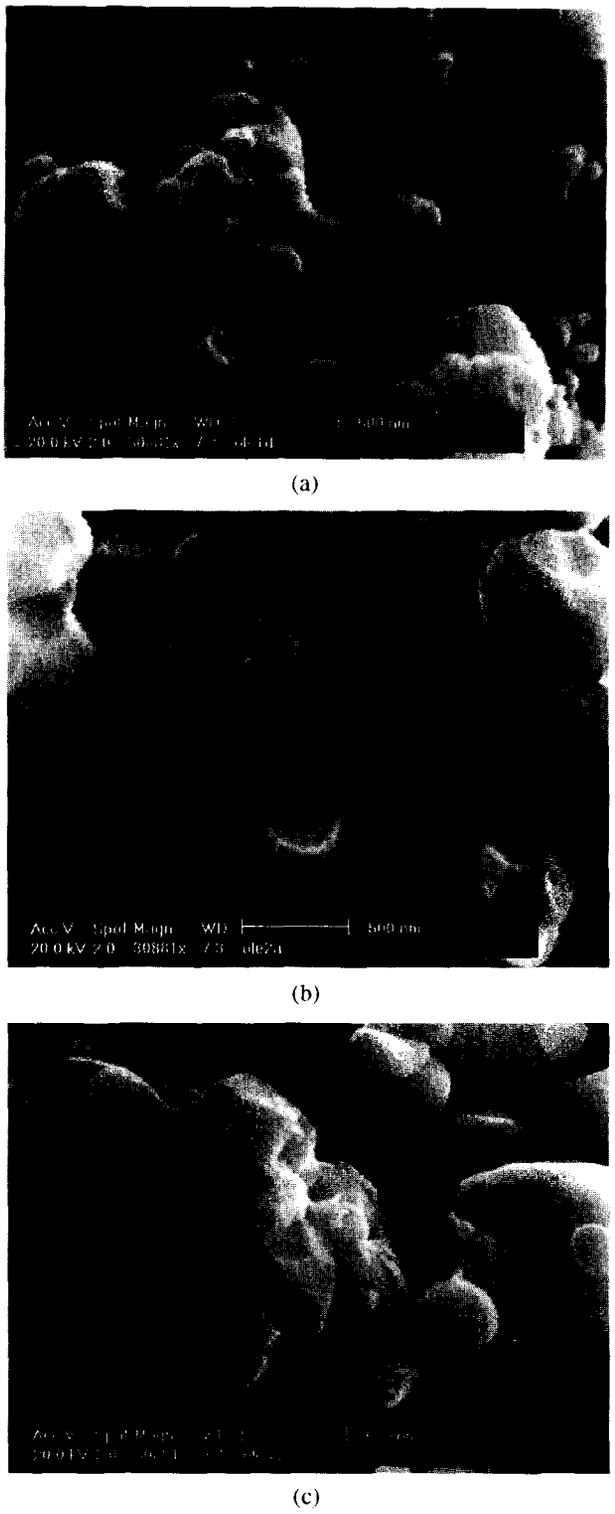

Fig. 5. SEM micrographs showing the particle morphology of batch Z1 calcined at (a) 850°C, 60 min (b) 850°C, 300 min and (c) batch Z2 calcined at 850°C for 300 min.

from approximately 100 nm (60 min.) to 160 nm (300 min.) in the Z1 mixture. In the Z2 mixture the particle size reached approximately 500–600 nm after 300 min soaking (Fig. 5). The values of particle size computed from the X-ray analysis and from direct observation by electron microscopy are in reasonably good agreement.

4 Discussion

Examination of the solid state reactions in the low temperature range from 500–600°C reveals a number of polymorphic phase transitions involving lead oxide. At room temperature lead monoxide can occur in two polymorphic forms, namely litharge, with a tetragonal crystal structure considered to be the low temperature form stable up to 500°C, and massicot, having an orthorhombic structure stable above 500°C. Being metastable at room temperature, massicot partially transforms during mechanical treatment (blending and grinding) to

litharge, the stable form at room temperature.[3,4] Indeed, traces of this phase were detected in the initial mixture before calcination. Heat treatment above 500°C causes transition of the metastable litharge to the stable massicot form. The other metastable phase observed was Pb_3O_4. This phase can be easily formed during heating of highly dispersed PbO in air at approximately 500°C and with further temperature increases it transforms back to PbO.[5]

The first traces of tetragonal $PbTiO_3$ phase were already detected at 550°C. A number of investigations performed on PZT-based systems showed the possibility of formation of this phase in the temperature interval 450–550°C.[6–12] It has been shown that, depending on the state of the TiO_2 powder (technological prehistory, morphology and surface area), reaction between PbO and TiO_2 can proceed very easily. Thus in a spray-dried PZT composition, formation of $PbTiO_3$ phase was observed at 430°C.[8] Comprehensive investigations of the ternary PbO–TiO_2–ZrO_2 system have shown clearly that the solid state reaction usually begins by the formation of tetragonal lead titanate solid solution, the residuals entering with a further increase in temperature.[6,7,9]

A substitution of Zr^{4+} for Ti^{4+} in $PbTiO_3$ reduces the tetragonal distortion and ultimately causes the appearance of another ferroelectric phase of rhombohedral R3m symmetry. Further development of new perovskite compositions based on polycomponent systems such as PbO–ZrO_2–TiO_2+(NiO, Nb_2O_5, MgO ....) did not show a retardation in the rate of formation of $PbTiO_3$ as the first phase during the calcination stage of mixed oxides.[10–12] For instance, investigations in the PbO–NiO–MgO–TiO_2–Nb_2O_5 system[11] revealed formation of the $PbTiO_3$ phase at approximately 600°C during calcination of precursors processed by a conventional oxide route. As expected, the $PbTiO_3$ was the primary phase formed also in the present investigation. This phase was a dominant phase within the range 600–700°C which agrees well with.[10–12] Above 700°C, the solubility of the residuals (Zr^{4+}, Nb^{5+} and Ni^{2+}) drastically changed the tetragonality of $PbTiO_3$, giving rise to the formation of a $PbTiO_3$ based solid solution with rhombohedraltype structure. It seems that the exothermic nature of the PbO + TiO_2 reaction facilitates the primary formation of the $PbTiO_3$ phase regardless of the complexity of the perovskite composition predicted in the morphotropic boundary.

The other dominating phase formed during calcination was a binary Pb–Nb-based compound. The formation of Nb-based phases proceeds via formation of the lead-rich tetragonal phase $Pb_3Nb_2O_8$, according to the following reaction:

$$3PbO + Nb_2O_5 \rightarrow Pb_3Nb_2O_8 \qquad (2)$$

Traces of this phase were found at the beginning of the calcination. Further progress of the reaction with increasing temperature above 550°C involved more Nb_2O_5 in the reaction with PbO, which promoted the formation of a rhombohedral phase based on $Pb_2Nb_2O_7$. The reaction can be written:

$$2Pb_3Nb_2O_8 + Nb_2O_5 \rightarrow 3Pb_2Nb_2O_7 \qquad (3)$$

This rhombohedral form showed a wide range of stability from 600–750°C and it was one of the main phases within this temperature interval. Raising the temperature above 700°C increased the solubility of Nb oxides in $Pb_2Nb_2O_7$ and led to formation of the cubic phase:

$$3Pb_2Nb_2O_7 + Nb_2O_5 \rightarrow 2Pb_3Nb_4O_{13} \qquad (4)$$

This sequence of solid state reactions coincides well with the phase diagram of the binary PbO–Nb_2O_5 system given by Roth.[13] According to this diagram, the binary compound transforms from tetragonal $Pb_3Nb_2O_8$ located on the PbO-rich side to rhombohedral $Pb_2Nb_2O_7$. In this case it is quite important to emphasise the variation in stoichiometry of the two compounds. The ratio of PbO to Nb_2O_5 changes from 3:1 (tetragonal symmetry) to 2:1 (rhombohedral symmetry). Increasing Nb–oxide content will change the stoichiometry and will lead to the formation of cubic $Pb_3Nb_4O_{13}$ with a ratio PbO to Nb_2O_5 of 1.5:1. The observed sequence in the formation of the pyrochlore phase demonstrates that the PbO species has a higher mobility than the other components.

The observed reaction sequence in the formation of the binary Pb–Nb-based compound in the present investigation appears somewhat different from the investigations presented in.[11,12,14–16] First of all, it should be mentioned that there are still different opinions as to the nature of the dominant pyrochlore phase. This question was first raised by Inada,[15] who pointed out the formation of cubic pyrochlore ($Pb_3Nb_4O_{13}$) within the range 530–600°C. Dambekalne[14] noted the formation of both rhombohedral ($Pb_2Nb_2O_7$) and tetragonal ($Pb_3Nb_2O_8$) phases in the range 550–700°C. Swartz and Shrout[12] proposed a sequence of solid state reactions in the PbO–Nb_2O_5–MgO system involving the formation of only one intermediate cubic pyrochlore phase. In spite of the apparent contradictions it has been agreed that the sequence of formation of pyrochlore phases depends very much on various experimental parameters such as particle size, surface state of raw materials and heating rates.[12] For example, Bouquin[16] clarified

the reaction sequence in a binary system model and found some differences with respect to the published phase diagram[13] and to multicomponent systems. In a Pb-rich ternary perovskite system Dambekalne[14] found coexisting rhombohedral and tetragonal pyrochlore phases with residual raw materials. Sasaki[11] identified the formation of $Pb_{14}Nb_{10}O_{39}$ up to 600°C in the complicated system PbO–NiO–MgO–TiO_2–Nb_2O_5. The latter results are quite similar to those of the present investigation. As far as the rhombohedral phase is concerned, it is recognised that, in most cases, it forms prior to the cubic pyrochlore.[14–16] It is also generally agreed that the latter is the high temperature form and that it is the basis for the formation of perovskite phases. The suggested sequence in the formation of the pyrochlore phases in the present investigation can be explained in terms of strong dependence of the ratio of the Pb/Nb constituents in a binary compound on the calcination temperature. This can be due to a number of factors. Firstly the complexity of the diffusion paths of species in multicomponent systems makes the process more sensitive to time–temperature variations. Another factor affecting the reaction sequence could by the mobility of the ionic species. It is likely that the high mobility of PbO determines the variation in stoichiometric compositions of pyrochlore phases.

The calcination is completed by the formation of the PZT–PNN solid solution. At 750°C the amount of this phase is approximately 30 wt%. Within the temperature interval 700–850°C it seems that the PZT–PNN is formed through mutual solubility of the $PbTiO_3$ and $Pb_3Nb_4O_{13}$ phases, whilst residuals ($PbZrO_3$ and NiO) are steadily dissolved in the formed solid solution. As a summary the final stage of the PZT–PNN formation can be presented as follows:

$$\left.\begin{array}{c} PbTiO_3 \\ + \\ Pb_3Nb_4O_{13} \\ + \\ PbZrO_3 \\ + \\ NiO \end{array}\right\} \Rightarrow Pb(Zr_{0.48}Ti_{0.52})O_3 - Pb(Ni_{1/3}Nb_{2/3})O_3$$

No peaks attributable to isolated PZT were observed. However, formation of small amounts of PZT cannot be ruled out, since interpretation of the X-ray patterns is difficult. Above the Curie temperature, the PT–PZ continuous solid solution forms perovskite with cubic crystal structure. Cooled to room temperature, the solid solution within the morphotropic phase boundary can exist in a tetragonal and a rhombohedral structure. As a result, XRD patterns are complex, involving overlaps and shifts of peaks due to solid solution formation.

One of the interesting results of this investigation is the clarification of the influence of the ZrO_2 particle size on the formation PZT–PNN solid solution. It is a well known fact that by adjusting the morphology and particle size of the constituents it is possible to affect the temperature and time of the calcination or sintering process. Thus the reduction of ZrO_2 particle size caused an increased rate of solubility of Pb–Zr–based residuals in the PZT–PNN solid solution. By increasing the surface area of the ZrO_2 particles the $PbZrO_3$ residuals were completely dissolved within 180 min. soaking time at 850°C. At the same time the large surface area activated the coarsening process sharply leading to a fivefold increase in linear grain size. It seems that the creation, in a powder system, of a high variation in surface area leads to fast grain growth.

5 Conclusion

The reaction sequence during the calcination of a perovskite with the composition $PbZrO_{0.48}Ti_{0.52}$–$PbNi_{1/3}Nb_{2/3}O_3$ (PZT–PNN) prepared by a conventional pure oxide mixture route has been investigated. It has been established that main phases formed prior to the perovskite were $PbTiO_3$ and Pb–Nb-based solid solution. The first traces of these phases were detected within the temperature 500–600°C.

The Nb-based pyrochlore phase was observed to gradually change its stoichiometry with increasing temperature. The sequence of pyrochlore formation was found to be from tetragonal $Pb_3Nb_2O_8$ (500°C) to rhombohedral $Pb_2Nb_2O_7$ (600–750°C) and finally to the cubic $Pb_3Nb_4O_{13}$ phase (650–850°C)

The formation of perovskite phase proceeds from mutual solubility of $PbTiO_3$ and $Pb_3Nb_4O_{13}$ phases accompanied by dissolution of the residuals ($PbZrO_3$ and NiO) in the solid solution formed. It was recognised that the sluggish solubility of cubic pyrochlore and $PbZrO_3$ phases would limit the homogeneity of the formed perovskite. However, complete solubility of $PbZrO_3$ was achieved by adjusting the morphology and the particle size of the ZrO_2 precursor.

Acknowledgements

The authors extend thanks to Professor Richard Warren for valuable advice and Dr Liu-Ying Wei for making the SEM-pictures. The work was carried

out as a part of the European COST 503 action entitled "Ceramic Materials for Piezoelectric Sensors and Actuators under Extreme Conditions".

References

1. Joffe, B., Roth, R. S. and Marzullo, S., Piezoelectric properties of lead zirconate-lead titanate solid-solution ceramics. *J. Appl. Phys.*, 1954, **25**, 809.
2. Klug, H. P. and Alexander, L. E., *X-ray Diffraction Procedure*. J. Wiley & Son, New York, 1974.
3. Senna, M. and Kuno, H., Polymorphic transformation of PbO by isothermal wet ball milling. *J. Am. Cer. Soc*, 1971, **54**(5), 259–262.
4. Chen, S. Y., Cheng, S. Y. and Wang, C. M., Polymorhpic phase transformation of lead monoxide and its influence on lead zirconate titanate formation. *J. Am. Cer. Soc*, 1990, **73**(3), 32–236.
5. Remi, H., *Lehrbuch der anorganischen chemie.*, Akad. Verlag., Leipzig, 1960.
6. Matsuo, Y. and Sasaki, H., Formation process of lead zirconate-lead titanate solid solutions. *J. Am. Cer. Soc*, 1965, **48**(6), 289–291.
7. Ikeda, T., Okano, T. and Watanabe, M., A ternary system PbO–TiO_2–ZrO_2. *Japan Applied Physics*, 1962, **1**, 218.
8. Dayal, R. and Prasad, C. D., Calcination characteristics of spray-dried PZT and related powders. *Mat. Res. Bull*, 1990, **25**, 1339–1346.
9. Chandratreya, S. S., Fulrath, R. M. and Pask, J. A., Reaction mechanisms in the formation of PZT solid solution. *J. Am. Cer. Soc*, 1981, **64**(7), 422–425.
10. Ng, Y. S. and Alexander, S. M., Structural studies of man ganese stabilised lead–zirconate–titanate. *Ferroelectrics*, 1983, **51**, 81–86.
11. Sasaki Y., Nagai A. and Yoshimoto T., Mechanism of PNN based perovskite ceramics formation, chemistry of electronic ceramic materials, Proceedings of the international conference held in Jackson WY, 1990, pp. 99–104.
12. Swartz, S. L. and Shrout, T. R., Fabrication of perovskite lead magnesium niobate. *Mat. Res. Bull*, 1982, **17**, 1245–1250.
13. Levin, E. M., Robbins, C. R. and McMurdic, H. F., Phase diagram for ceramists. *Am. Cer. Soc. Inc.*, Columbus, 1964, 117.
14. Dambekalne, M., Brante, I. and Sternberg, A., The formation process of complex lead-containig niobates. *Ferroelectrics*, 1989, **90**, 1–14.
15. Inada, M., Analysis of the formation process of the piezoelectric PCM ceramics. *Natl. Tech. Rep*, 1977, **27**(1), 95–102.
16. Bouquin, O. and Lejeune, M., Formation of the perovskite phase in the $PbMg_{1/3}Nb_{2/3}O_3$–$PbTiO_3$ system. *J. Am. Cer. Soc*, 1991, **74**(5), 1152–1156.